Table 1. Standard percentage deviation of the experimental values of the heat transfer coefficient from the predicted values

Tube number	Outer diameter of tube (mm)	Percentage standard deviation from equation (7) (%)	Percentage standard deviation from equation (2) (%)
1	15.9	4.32	1.86
2	12.7	6.76	7.85
3	9.5	9.20	9.34
Overall		7.42	7.80

exponent has been determined as 0.86. Accordingly

$$\frac{h_{fb}}{h_f} = \left[1 + \left(\frac{h_b}{h_f}\right)^{0.86}\right]^{1.163}. \quad (7)$$

Figure 3 shows the plot of the heat transfer coefficient h_{fb} obtained by the above correlation against the experimental data. On the same plot a comparison of h_{fb} has been made with the one obtained by equation (2). It is found from this plot that the values predicted by the two equations do not differ appreciably from the experimental values. However, the predicted 'h' values obtained by equation (7) show only marginal superiority. Table 1 has been prepared to show the standard percentage deviation of the values of the experimental heat transfer coefficient from those predicted by equation (7) as well as equation (2).

REFERENCES

1. W. C. Elrod, J. A. Clark, E. R. Lady and H. Merte, Boiling heat transfer data at low heat flux, *Trans. Am. Soc. Mech. Engrs*, Series C, *J. Heat Transfer* 89, 235 (1967).
2. R. M. Fand, K. K. Keswani, M. M. Jotwani and R. C. C. Ho, Simultaneous boiling and forced convection heat transfer from a horizontal cylinder to water, *Trans. Am. Soc. Mech. Engrs*, Series C, *J. Heat. Transfer* 98, 395 (1976).
3. G. C. Vliet and G. Leppert, External flow, *Adv. Heat Transfer* 1, 245 (1964).
4. H. R. McKee and K. J. Bell, Forced convection boiling from a cylinder normal to the flow, *Chem. Engng Prog. Symp. Ser.* 92(65), 222 (1969).
5. S. S. Kutateladze, Boiling heat transfer, *Int. J. Heat Mass Transfer* 4, 31 (1961).
6. W. M. Rohsenow, Heat transfer—a symposium, Engineering Research Institute, University of Michigan (1952).
7. K. Engelberg-Forster and R. Greif, Heat transfer to boiling liquid—mechanism and correlations, *Trans. Am. Soc. Mech. Engrs*, Series C, *J. Heat Transfer* 74, 969 (1952).
8. W. M. Rohsenow, A method of correlating heat transfer data for surface boiling of liquids, *Trans. Am. Soc. Mech. Engrs*, Series C, *J. Heat Transfer* 74, 969 (1952).
9. S. S. Kutateladze and V. M. Borishanskii, *A Concise Encyclopaedia of Heat Transfer*, p. 202. Pergamon Press, Oxford (1966).
10. C. P. Gupta and R. Prakash, *Engineering Heat Transfer*, p. 266. Nem Chand and Bros., Roorkee, India (1976).

Int. J. Heat Mass Transfer. Vol. 26, No. 12, pp. 1885–1889, 1983
Printed in Great Britain

0017-9310/83 $3.00 + 0.00

THE EFFECT OF A MAGNETIC FIELD ON THE HEAT TRANSFER CHARACTERISTICS OF AN AIR FLUIDIZED BED OF FERROMAGNETIC PARTICLES

JULIE J. NEFF and BORIS RUBINSKY*

Department of Mechanical Engineering, University of California, Berkeley, CA 94720, U.S.A.

(*Received* 12 *October* 1982 *and in revised form* 1 *March* 1983)

NOMENCLATURE

- A_s effective area of the heat transfer probe [m^2]
- B magnetic flux density [gauss]
- d_p average particle diameter [m]
- h heat transfer coefficient [W m^{-2} K^{-1}]
- T_b bulk bed temperature [K]
- T_s probe surface temperature [K]
- u airflow velocity [m s^{-1}]
- u_{mf} minimum fluidization airflow velocity [m s^{-1}].

INTRODUCTION

A GAS–SOLID fluidized bed contains a bed of particulate matter through which a gas (air) is passed. As the airflow rate increases, four fluidized regimes can be observed; namely, the fixed bed, incipient fluidization, bubbling and slugging regimes [1–5]. It has been shown that the heat transfer is different in the four different fluidization regimes [2, 5]. The region of low air velocity corresponding to the fixed bed regime is characterized by low heat transfer coefficients. The incipient fluidization regime is characterized by a gradual increase in the heat transfer coefficients with maximal heat transfer occurring in the bubbling regime. The slugging regime is accompanied by a decrease in the heat transfer coefficient.

Recent investigations have shown that electrical fields can effect the fluid flow mechanics in fluidized beds of insulating and semi-insulating particles and consequently the heat transfer [6–8]. It has also been reported by Agbim *et al.* [9] that the fluidized bed regimes were changed when fluidizing magnetized iron shots. The onset of bubbling was suppressed and the bed stabilized when fluidizing magnetic iron shots as compared to the fluidization of iron shots of the same size but not magnetic.

This note documents the effect of an applied exterior magnetic flux on the flow regimes and heat transfer from a vertical flat surface in a fluidized bed of ferromagnetic

* To whom correspondence should be addressed.

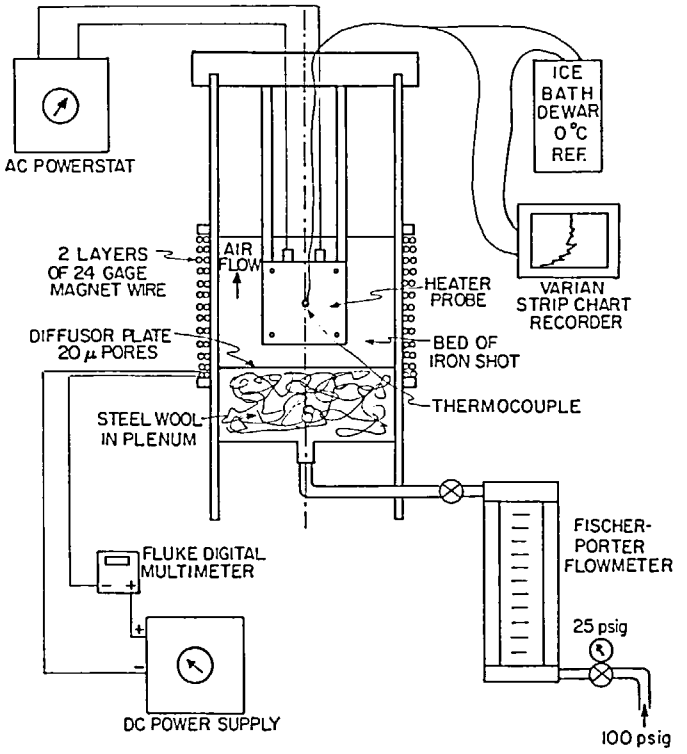

FIG. 1. Schematic of the experimental setup.

particles. The experimental data indicates that the fluidized bed of ferromagnetic particles exhibits, in the presence of a magnetic field, the same regimes as the bed in the absence of the magnetic field (fixed bed, incipient fluidization, bubbling) but that the incipient fluidization occurs at higher airflow velocities with an increase in the magnetic field.

EXPERIMENTAL SYSTEM AND PROCEDURE

The experimental system consists of a cylindrical Plexiglas chamber containing a bed of iron particles and a heater heat transfer probe. The outside of the chamber is wound with a solenoidal electromagnet. Additional components of the system are power and compressed air supplies, and data acquisition instrumentation. The schematic of the system is shown in Fig. 1.

The inner diameter of the chamber is 8.89 cm and the chamber height is 33.2 cm. At the bottom of the chamber is a 20 μm pore diameter steel distributor plate. The fixed, or unfluidized bed height is constant at 10.48 cm. The air entry port is supplied with compressed air maintained at a constant operating pressure of 25 psig. The particle matter used in the bed is iron chilled shot. The mean diameter, d_p was found to be 0.727 mm by using the formula recommended by Botterill [5]:

$$d_p = \left[\sum_i (x_i/d_{pi})\right]^{-1}. \quad (1)$$

The heat transfer probe consists of an electrical thermo-foil resistance heater mounted between two plates (4.45 × 3.81 × 0.16 cm). The probe is oriented vertically in the bed with its center located 4.6 cm above the distributor plate. A copper–constantan thermocouple is mounted on the aluminum plate. The electromagnet is a two layer solenoid of 24 gage copper magnet wire with enamel insulation. It begins just below the distributor plate and extends to 10.5 cm above the plate. It is supplied with current by a DC stabilized power supply.

Experiments were conducted to determine the heat transfer coefficients from the vertical flat surface immersed in a fluidized bed. Two parameters were varied, the airflow velocity and the magnetic field strength, or magnetic flux density. During each test, four quantities were measured—volumetric airflow rate, DC current supplied to the windings, the power supplied to the probe, and the probe temperature. These raw data were then converted to the parameters of interest—air velocity, magnetic flux density, and heat transfer coefficient.

The experimental airflow velocities used ranged from 0.91 to 1.24 m s^{-1}. The measurement uncertainty is ± 0.01 m s^{-1}.

The magnetic field was measured using a RFL Model 1890 gaussmeter. A current was applied to the electromagnet of the fluidized bed, and was monitored with a Fluke 8020A multimeter. The current was varied from 0 to 1500 mA, and the magnetic flux density was found to vary linearly with the current from 0 to 45.7 gauss (4.57×10^{-3} T). Experimental uncertainty is ± 0.2 gauss. To investigate the variation of flux density within the bed, the gaussmeter probe was inserted into the middle, top, and bottom of the fixed bed (locations at 1.3, 5.2, and 9.2 cm from the top of the distributor plate). The fluxes at the top and bottom of the bed were $25 \pm 3\%$ less than the flux in the middle. All reported values of magnetic flux density will refer to the middle of the bed.

The thermocouple on the heater probe, in the absence of heating, provided the temperature of the fluidized bed, T_b. During each test the heater was switched on providing a constant, known heat source q. The probe temperature, T_s, was then allowed to reach steady state for current levels through the magnet from 0 to 1500 mA at 100 mA increments. The heat transfer coefficient is thus determined:

$$h = \frac{q}{A_s(T_s - T_b)}. \quad (2)$$

Typical values for T_s and T_b were 60 and 30°C, respectively.

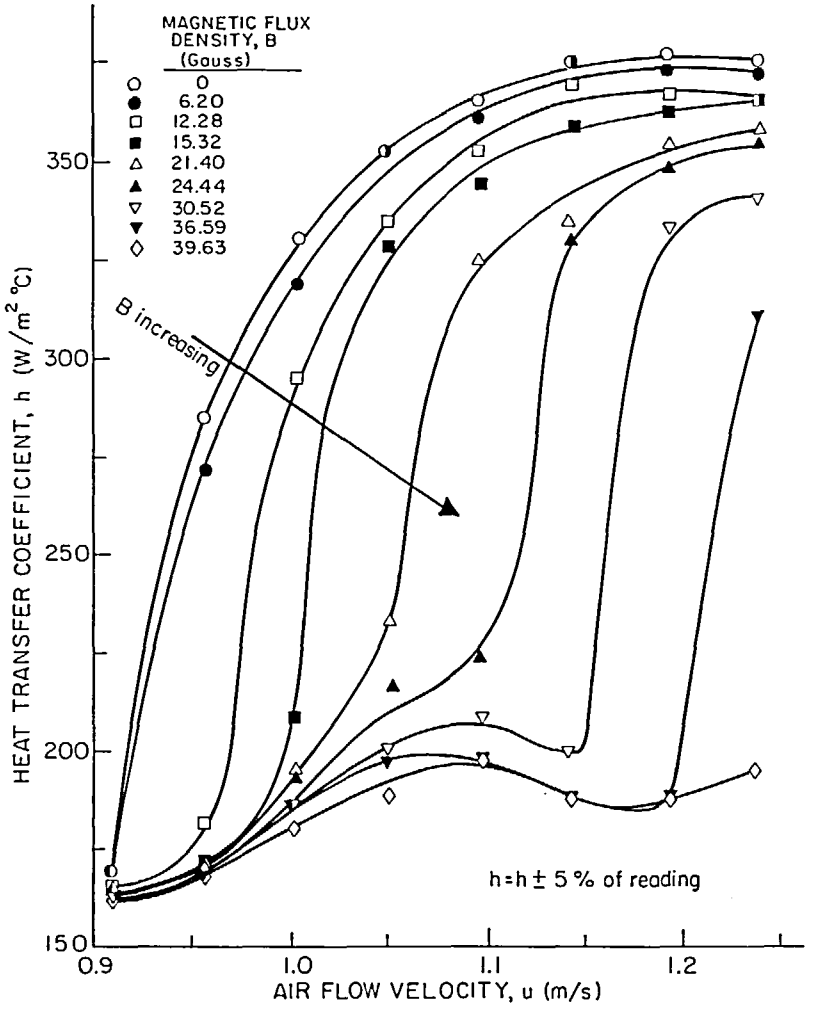

FIG. 2. Heat transfer coefficients as a function of airflow velocities for various magnetic flux densities.

The effects of radiation heat transfer can be neglected in the interpretation of the results. During all the experimental runs, reported here, the magnetic field direction vector was pointing in the positive y direction (gravity vector is assumed to be pointing in the negative y direction).

RESULTS AND DISCUSSION

Heat transfer measurements were made for 15 different values of magnetic flux densities at eight different air velocities. Results of these runs are plotted as heat transfer coefficients vs airflow velocity curves for ten values of the magnetic flux density, B, in Fig. 2. Each curve exhibits the fluidization regimes discussed in the introduction, i.e. fixed bed, incipient fluidization and bubbling. In general, the typical curves shift to the right as the magnetic flux density is increased. The curves show the visual observations that incipient fluidization occurs at higher airflow velocities for larger magnetic fluxes. For a given magnetic flux an increase in the airflow velocities will cause initially a slight increase in the heat transfer coefficient although the bed retains a fixed bed appearance. This is caused by the increased air convection heat transfer. It is seen that for each magnetic flux there is a 'critical' narrow region of airflow velocities at which the heat transfer coefficients drop off drastically with a decrease in airflow velocity. This phenomena is referred to in this work as the onset of 'freezing' of a fluidized bed. The flow modes are very unstable at these critical airflow velocities and bubbling starts and stops very intermittently.

The 'critical' airflow velocity, u_{mf}, was plotted as a function of the magnetic flux density, B, in Fig. 3. The specific value for the critical airflow velocity has been chosen to be the lower limit of the range of airflow velocities in which the dramatic change in heat transfer coefficients occurs when a constant magnetic flux B is applied on the fluidized bed. It is interesting to notice that the relation is linear. This linear relation can be expressed through the linear regeneration curve fit obtained from Fig. 3. The expression correlates the incipient 'critical' fluidization airflow velocity, u_{mf}, with the magnetic flux B

$$B_c = -86.55 + 102.44 u_{mf}, \tag{3}$$

where B_c is in gauss and u_{mf} in m s^{-1}.

A ferromagnetic particle in the fluidized bed is probably effected by four different forces, the drag force, gravity, interparticular magnetic forces and forces which the exterior magnetic field applies on a particle. In the absence of magnetic forces the airflow drag force has to be equal to the weight of the particle for fluidization to start. The experimental results suggest that as the airflow is increased in a fluidized bed of ferromagnetic particles, the drag force would first overcome gravity and particles will start to levitate. A further increase in the airflow will cause an expansion of the fluidized bed with particles held in place by the inter-particle magnetic force.

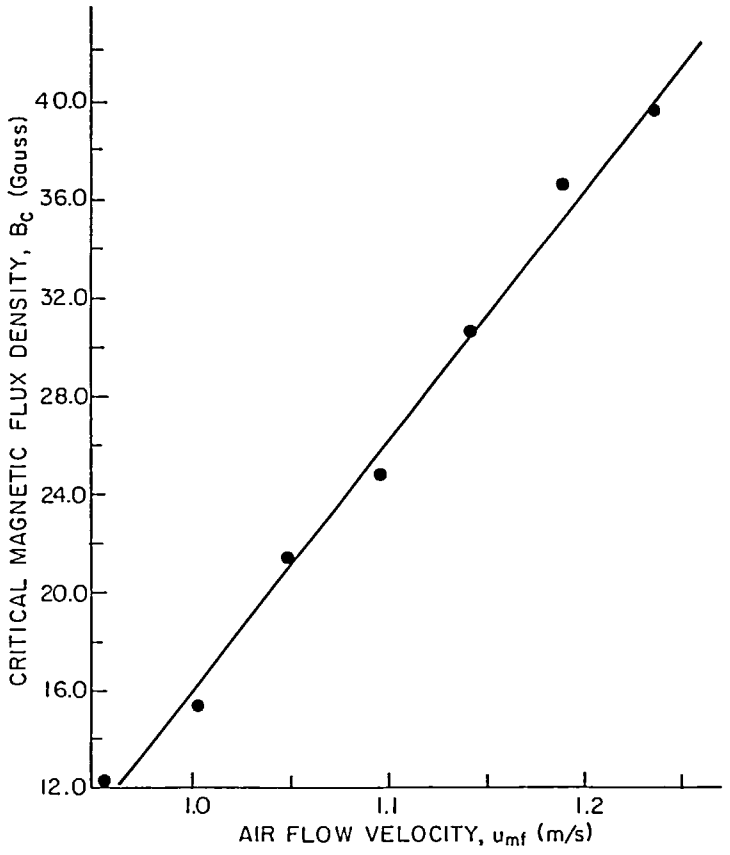

FIG. 3. Critical magnetic flux density as a function of velocity.

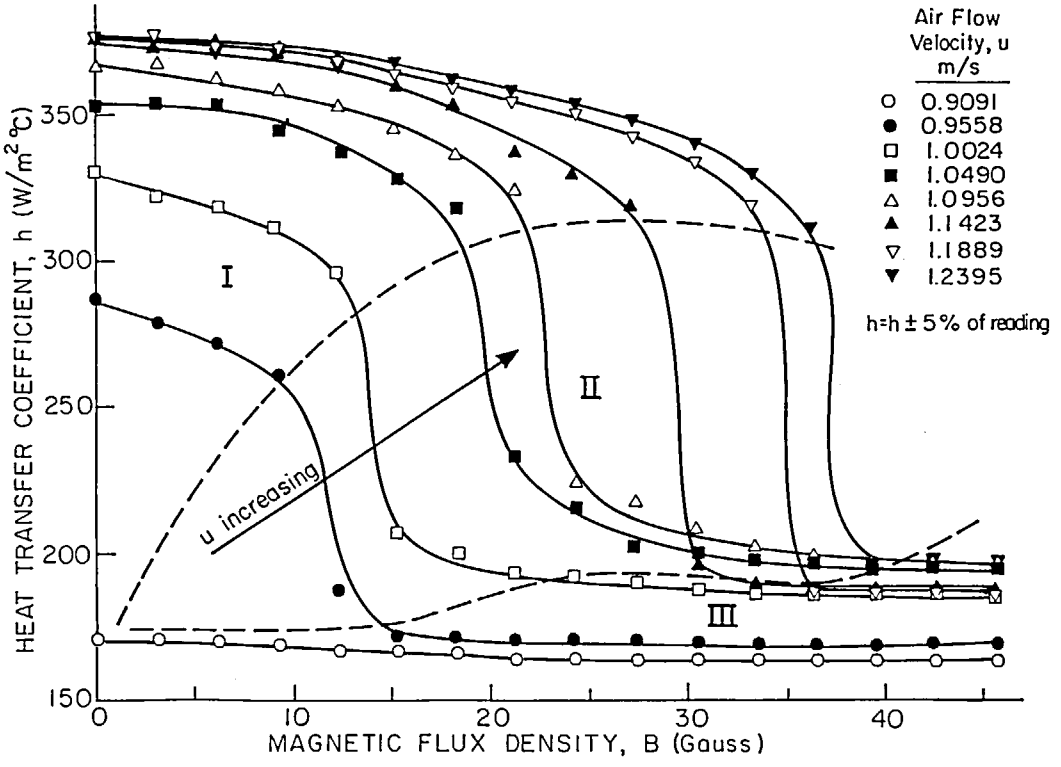

FIG. 4. Heat transfer coefficients as a function of magnetic flux density.

Experiments show that prior to the onset of fluidization the bed behaves actually as a fluid, i.e. it presents a flat upper surface, it presents a very small resistance to an object moving in the fluidized bed, disturbances (waves), generated on the surface decay. Fluidization, vigorous movement of particles will occur when the airflow drag forces can overcome the stabilizing force of the exterior magnetic field which tends to maintain particles stationary. This has been shown in Fig. 3.

A different presentation of the results is shown in Fig. 4. Figure 4 shows the heat transfer as a function of magnetic flux density at various velocities. There are, in effect, three regimes in which magnetic field relative strength, i.e. as compared to velocity, can be classified. The first regime is a low field linear regime. The second is the onset of freezing at medium field strengths. The third is the fixed bed regime at high field strengths.

The low field regime exhibits a slight and quite linear reduction in heat transfer coefficient. In this regime, there are no observable characteristics. The inter-particle forces are small, probably alter non-observable flow patterns and reduce bubble size. The decrease in heat transfer is probably caused by those inter-particle forces.

The onset of 'freezing' is characterized by a large drop in heat transfer. Particle motion and bubbling can be seen to be greatly reduced. This is especially evident for the high flow velocities. The great reduction in particle motion increases particle residence time at the probe surface and thus reduces heat transfer.

The third regime is the fixed bed regime. This is the regime in which all particle motion stops. The heat transfer coefficient is constant as magnetic flux density is increased, and is determined by the voidage patterns established throughout the fluidized bed in the previous regime and the airflow velocity. In essence, the third regime is like the point of minimum fluidization in an unmagnetized bed. The bed exhibits fluidic characteristics and is expanded from the fixed bed state. It is more stable than the point of minimum fluidization in an unmagnetized bed, however. This is demonstrated when a perturbation to the system, such as shaking the bed, is damped out immediately; whereas, in an unmagnetized expanded bed a perturbation can cause slight bubbling. A perturbation in this regime will re-establish voidage patterns and can change the heat transfer coefficient up to a value as much as 7%.

Experiments in which the polarity of the magnetic field, i.e. the direction of the DC current flow was reversed do not indicate any effect of the polarity on heat transfer.

CONCLUSIONS

Heat transfer coefficients for a flat vertical probe in a bed of ferromagnetic particles were measured in the presence of a magnetic field. Results indicate that heat transfer is reduced as magnetic field strength is increased. The minimum fluidization velocity and the entire heat transfer vs airflow velocity curve shifts to higher velocities as the field strength is increased. The shift is caused by the need to increase the airflow drag forces to overcome the exterior field magnetic forces at the onset of fluidization.

The potential for control of fluidized bed dynamics and heat transfer processes by introducing a magnetic field is very evident in this study.

REFERENCES

1. M. Leva, *Fluidization*. McGraw-Hill, New York (1959).
2. S. S. Zabrodsky, *Hydrodynamics and Heat Transfer in Fluidized Beds*. MIT Press, Cambridge, Massachusetts (1966).
3. D. Kunii and O. Levenspiel, *Fluidization Engineering*. Wiley, New York (1969).
4. P. N. Rowe, *Fluidization* (edited by J. F. Davison and D. Harrison), pp. 121–191. Academic Press, London (1971).
5. J. S. M. Botterill, *Fluidized Bed Heat Transfer*. Academic Press, New York (1975).
6. R. Elsdon and C. J. Shearer, Heat transfer in a gas fluidized bed assisted by an alternating electric field, *Chem. Engng Sci.* **32**, 1147–1153 (1977).
7. P. W. Dietz, Heat transfer in bubbling electrofluidized beds, *Proc. Symp. on Electrohydrodynamics*, Fort Collins, Colorado (1978).
8. H. Katz and J. T. Sears, Electric field phenomena in fluidized and fixed beds, *Can. J. Chem. Engng* **47**, 50–53 (1969).
9. J. A. Agbim, A. W. Nienow and P. N. Rowe, Interparticle forces that suppress bubbling in gas fluidized beds, *Chem. Engng Sci.* **26**, 1293–1295 (1971).

Int. J. Heat Mass Transfer. Vol. 26, No. 12, pp. 1889–1892, 1983
Printed in Great Britain

0017-9310/83 $3.00 + 0.00

MIXED CONVECTION HEAT TRANSFER FROM A VERTICAL HEATED CYLINDER IN A CROSSFLOW

M. F. YOUNG and T. R. ULRICH
Department of Mechanical Engineering, University of California, Irvine, CA 92717, U.S.A.

(*Received* 27 *January* 1983 *and in revised form* 4 *April* 1983)

NOMENCLATURE

A	surface area
c_p	specific heat
d	diameter or differential
g	acceleration of gravity
Gr_L	Grashof number based on $L = \beta g(T_W - T_\infty)L^3/\nu^2$
k	thermal conductivity
L	height
m	mass
Nu_d	Nusselt number based on d
$\overline{Nu}_d$	average Nusselt number based on d
Pr	Prandtl number
$\dot{Q}$	heat transfer rate
Re_d	Reynolds number based on $d = U_\infty d/\nu$
Ri	Richardson number, Gr_L/Re_d^2
t	time
T	temperature.

Greek symbols

β	coefficient of thermal expansion
Δ	finite difference
ε	emissivity
σ	Stefan–Boltzmann constant
ν	kinematic viscosity.